

Secular Variation of Activity in Comets 2P/Encke and 9P/Tempel 1

Michael Haken and Michael F. A'Hearn

Department of Astronomy, University of Maryland, College Park, Maryland 20742

Paul D. Feldman

Department of Physics and Astronomy, Johns Hopkins University, Baltimore, Maryland 21218

Scott A. Budzien

E.O. Hulbert Center for Space Research, Naval Research Laboratory, Washington, D.C. 20375

Abstract

We compare production rates of H₂O derived from International Ultraviolet Explorer (IUE) spectra from multiple apparitions of 2 comets, 2P/Encke and 9P/Tempel 1, whose orbits are in near-resonance with that of the Earth. Since model-induced errors are primarily a function of observing geometry, the close geometrical matches afforded by the resonance condition results in the cancellation of such errors when taking ratios of production rates. Giving careful attention to the variation of model parameters with solar activity, we find marginal evidence of change in 2P/Encke: a 1- σ pre-perihelion decrease averaging 4%/revolution over 4 apparitions from 1980-1994, and a 1- σ post-perihelion increase of 16%/revolution for 2 successive apparitions in 1984 and 1987. We find for 9P/Tempel 1, however, a 7- σ decrease of 29%/revolution over 3 apparitions from 1983-1994, even after correcting for a tracking problem which made the fluxes systematically low. We speculate on a possible association of the character of long-term brightness variations with physical properties of the nucleus, and discuss implications for future research.

1 Introduction

Secular variations in comets may be important indicators of physical properties or processes which are inaccessible to direct scrutiny, but they may themselves be rather difficult to detect. However, comets with particularly short orbital periods may reveal evidence of secular changes with an observational baseline of relatively modest length. In fact, in the classic case of the comet with the shortest known period, 2P/Encke ($P \sim 3.3$ yr), it was only 33 years, with four observed apparitions, before the apparent secular acceleration in

its orbital motion led J.F. Encke to invoke for the first time a concept with far-reaching physical implications: that comets may experience non-gravitational forces.¹

Although the correct interpretation of the effect - recoil of a solid nucleus from ejected mass - was given by Bessel in 1836, the significance of Encke's discovery was essentially lost for over a century. The supposition that comets are swarms of small bodies, implicit in Encke's own "resisting medium" hypothesis, became virtual dogma once the association of meteor streams with cometary orbits was recognized in the 1860s.² Bessel's insight was restored with phenomenal success in 1950 with Whipple's now-canonical model of the cometary nucleus as a solid body of low density and low thermal conductivity. While the empirical basis of this icy conglomerate, or "dirty snowball", model was the non-gravitational component of 2P/Encke's motion, the reality of the small (≤ 0.1 day/(revolution)²) effect was disputed even into the 1960's (Marsden 1967). Only with the application of high-speed, high-precision computers was the existence of both secular accelerations and decelerations in the motions of short-period comets conclusively demonstrated (Marsden 1968).

By modeling the observed orbital acceleration as a consequence of volatiles sublimed from a retrograde-rotating nucleus, with maximum outgassing displaced beyond the subsolar point due to thermal inertia, Whipple deduced a mass loss rate $\Delta M/M \sim (0.2-0.5)\%/revolution$. While the decline in mass is not itself directly observable, the assumption that a comet's activity level will be correlated with its mass leads one to postulate a systematic decline in activity, at least if long enough time scales are considered. Yet the supposition that the process will be one of monotonic decline, perhaps nearly inescapable for a comet on a stable orbit if one accepts the "meteor swarm" model, is clearly too simplistic. The irregular topography and apparent localization of outgassing seen at the surface of 1P/Halley (Keller et al. 1986) suggest that modulation of activity may be quite complex. Even within a given active region, volatiles may not be uniformly distributed, and activity may be mediated by processes independent of the mass of volatiles, such as mantle build-up or blow-off, which may affect outgassing discontinuously. Such surface processes, along with possible heterogeneous nuclear morphologies and changes in insolation patterns from orbital or orientational evolution, may mean that cycles of dormancy and re-activation are the rule rather than the exception. Indeed, 2P/Encke, which despite a highly stable orbit was apparently never seen prior to 1786, may have been discovered after emerging from an extended period of dormancy (Sekanina 1991).

Progressive fading has nonetheless been claimed for 2P/Encke and several other short-period comets, but has never been convincingly demonstrated. Virtually all previous work has been based on visible magnitude estimates spanning a century or more and obtained

¹Historical background material from Sekanina, 1991.

²An amusing illustration of the tenacity of such flawed paradigms is found in the 1937 *Encyclopedia Britannica*. A.C.D. Crommelin, a former president of the R.A.S and highly reputed for orbital work on the comet which bears his name, posits "there are two ways in which comets may cease to exist as such. Either the meteors in the head may lose all their gas...or the meteors may become so diffuse and scattered as to lose all semblance of unity and coherence", even though he admits "we have no experience of the dissolution of a comet in the latter sense". He has difficulty reconciling the fact that "comet Pons-Winnecke...has made several close approaches to Jupiter; further it has given rise to a meteor shower which was well seen in June, 1916" with the observation, "when the comet approached very near the Earth in June, 1927, its nucleus was seen to be very small, not more than 2 km in diameter", and thus concludes, "the coherence of the heads of some comets is surprisingly great, and seems to indicate some unknown force holding the constituents together."

using a wide range of naked-eye, telescopic, photographic, and photometric techniques. While the extreme inhomogeneity of these datasets makes any conclusions highly problematic, the data have nevertheless led to several claims of severe constraints on the physical lifetimes of short-period comets. If one assumes a quasi-steady state population, such constraints would have important implications for possible replenishment channels and origin scenarios. Even were monotonic fading of a comet confirmed, only a simplistic and probably unrealistic model of the nucleus could directly convert the fading rate into a lifetime. However, one would expect that the evolution of a comet’s activity in principle encodes information on the evolution and morphology of the surface, and possibly on the lifetimes and morphology of individual sources, although it is far from clear how one might begin to read such a code. It is first necessary learn whether any comets exhibit real trends of secular activity, and in which respects such comets may differ from those varying more erratically.

Until fairly recently, there was no clearly reliable way to index relative activity from apparition to apparition. The index we adopt here, based on the production rate of water, is the natural index of activity, since water is the volatile believed to drive the activity of comets at $r \lesssim 3$ AU. At these distances, cometary comae are rich in OH, which is produced almost exclusively by H₂O dissociation and which has strong transitions in the near-UV. Modeling of the coma, necessary to convert observed OH brightnesses to production rates, requires parameters which depend on heliocentric distance and assumes that the observed brightness is independent of observing geometry. To most confidently interpret the results, therefore, one should compare observations at identical comet-Earth-Sun configurations. If a cometary orbit is in near resonance with the Earth’s orbit, the geometry will repeat after an integral number of revolutions. Comets which possess short-term resonances, such as 2P/Encke and 9P/Tempel 1, are the best candidates for such comparisons. Of course, a uniform dataset spanning multiple apparitions is a prerequisite for meaningful results. One should expect to find the highest degree of uniformity in datasets collected by a well-calibrated space based instrument. The International Ultraviolet Explorer (IUE) ultraviolet spectrometer has observed 2P/Encke, with geometry approximately repeating every 3 revolutions, at 5 consecutive apparitions, and has observed 9P/Tempel 1 ($P \sim 5.5$ yr), with geometry almost exactly repeating every 2 revolutions, at 2 apparitions spanning 2 revolutions. IUE has obtained data which constrain relative brightnesses with high precision, and careful modeling of the data allows us to constrain changes in activity.

2 Previous Results

The problem of secular variation in the brightness of periodic comets dates back at least to the 1927 work of Vsekhsvyatskij, and has been the subject of much controversy, largely centered on 2P/Encke. Most authors have relied on visual magnitude estimates from extensive catalogs compiled by Vsekhsvyatskij, but with a great deal of disagreement over how to treat the data. The difficulty is twofold: 1) how to reduce estimates obtained at different epochs, and by a multitude of observers and techniques, to a common standard; and 2) how to best characterize the relative activity level at each apparition.

The first question is often referred to under the heading of “instrumental effects”, but encompasses not only differences between naked-eye and instrumental techniques, but also in observing geometry, sky brightness, and the subjective judgment of visual observers.

While he recognized this problem, Vsekhsvyatskij (1930) chose to skirt it, apparently reasoning that such errors would average out for a large enough sample. He suggested that a simple answer to the second question would be to compare only measurements made at the same r (although he made no distinction between pre- and post-perihelion phases, a serious error in light of current knowledge), but thought that poor statistics would then make the result very sensitive to the instrumental errors. He thus chose to base his comparison on a single index abstracted from all observations at a given apparition: the so-called “absolute magnitude”, defined to be the hypothetical observed magnitude for a comet at heliocentric and geocentric distances of 1 AU. Although aware that light curves differ from comet to comet and may deviate significantly from a simple power law for a given comet, he adopted for his definition of absolute magnitude a common simple dependence on distances r (heliocentric) and Δ (geocentric) for all comets. Assuming a Δ^{-2} law, he found that data for the majority of his sample could be approximately fit by an r^{-4} dependence, and thus arrived at the often quoted formula,

$$H_{10} = m - 10 \log r - 5 \log \Delta$$

where m is the observed magnitude and H_{10} is the magnitude inferred at $r = \Delta = 1$.

Vsekhsvyatskij (1929) claimed that values of H_{10} from 100 years of uncorrected 2P/Encke data “show the indisputable decrease of the comet’s brightness with time”, at a rate of 1.0 magnitudes/century or 0.033 magnitudes/revolution, corresponding to a relative brightness change of 3%/revolution. This assertion was immediately challenged by Koslov (1929), who held that the “insufficient exactness and small number” of data “do not permit any final statistical solution of the question concerning the long variation of brightness of the comet”. Undaunted, Vsekhsvyatskij (1930) extended the analysis to a sample of 12 short-period comets with an average period of 6.9 years, for which he found a mean fading rate of about 5 magnitudes/century or 0.35 magnitudes/revolution, an average decline in brightness of 17%/revolution. Convinced of the fundamental implications of his work, he remarks, “The question as to the origin of short-period comets (and perhaps of all comets) according to this investigation must now be taken up in a new way. *We must seek for the sources out of which these objects have been formed within the limits of our solar system*”. The italics are his.

Much of the subsequent work assumed Vsekhsvyatskij’s light curve, but differences in sampling and modeling the data and in treating instrumental effects led to a divergence of results.

Bobrovnikoff (1941) identified several possible sources of systematic error in Vsekhsvyatskij’s data, notably differences in methods based on stellar comparison for estimating magnitudes, differences in the effect of sky conditions on stellar and diffuse light, and an effect due to the aperture of the instrument used, which he found to be strongly correlated with the reported magnitude. Applying a formal correction based on telescope aperture only, Bobrovnikoff (1942) reported finding no evidence of fading in a sample of 45 comets, although it did not include 2P/Encke.

Whipple (1964) on the other hand, incorporating newer uncorrected data from Vsekhsvyatskij’s massive 1958 compendium, reached a startlingly different conclusion, predicting the demise of 2P/Encke and 7 other short period comets by the end of the century, and of 1P/Halley by 2458. Extrapolating backwards, he expressed the hope, yet unfulfilled, of finding reference to 2P/Encke and associated “phenomenal” meteor showers in an-

cient Chinese or Babylonian records. Whipple and Douglas-Hamilton (1966) found that correcting the data had little effect on the conclusion. Applying an aperture correction similar to Bobrovnikov's as well as a fixed correction for photographic observations, they fit the 2P/Encke data to a model of a homogeneous spherical nucleus losing a constant depth of material per revolution, and obtained a curve on which the rate of fading accelerates from around 1 magnitude/century in 1800 to nearly 5 magnitudes/century in 1950 - still in the relatively flat region! When the slope becomes a virtual cliff after 1975, one must conclude that the comet's days are truly numbered; in fact the "Death Date" of the model - when the radius goes to zero - is A.D. 2000. While their simplistic model is almost certainly incorrect, the data too are suspect.

Other proponents of an accelerating fading rate and early death date for 2P/Encke (~ 3 magnitudes/century and A.D. ~ 2050) included Sekanina (1964, 1972), from physical modeling of the nucleus, and Ferrin and Gil (1986), from a set of only naked-eye observations corrected for twilight effects. By this time Vsekhsvyatskij (1958) had revised his fading rate for 2P/Encke to over 2 magnitudes/century and the sample average to over 6.5 magnitudes/century, and was led to conclude, "the data gathered . . . prove the most important proposition of cometary astronomy, that comets disintegrate rapidly. We can only conclude that the age of short-period comets is measured in centuries, if not decades".

Others disputed such steep rates of fading. Kresák (1974) pointed out that they would imply (1) such rapid depletion that, if current thinking on origin and dynamical evolution is correct, the entire class of short-period comets would cease to exist within a few hundred years,³ (2) death dates for several comets which were at odds with more recent observations, and (3) high past brightnesses contradicting the absence of ancient and medieval records. He claimed that up to 80% of the apparent secular change could be explained by instrumental effects, which tend to increase with time, explaining the apparent acceleration of fading rates, and part of the remainder by selection effects such as the likelihood that a discovery apparition will be anomalously bright and a missed one anomalously faint. Kresák further pointed out that a correction based on aperture alone is too simplistic, as instrumental errors must depend on other factors, such as magnification, as well. Kresák and Kresáková (1986) proposed to reduce instrumental errors by selecting for comparison only the lowest H_{10} from each apparition, after applying to the apparent magnitudes a purely empirical correction, which brightened all reported magnitudes greater than 9, independent of observing technique. This approach seems somewhat paradoxical given that instrumental uncertainties are correlated with apparent, not absolute, magnitudes, and resulted in their rejecting some of the best data in favor of noisier data. Reevaluating the whole of Vsekhsvyatskij's sample, Kresák and Kresáková (1990) identified statistically significant fading trends for 7 comets, including 2P/Encke and 4 others singled out by Whipple, but with a maximum fading rate in their group of 0.18 magnitudes/revolution. To 2P/Encke they attributed the minimum rate in the group, 0.03 magnitudes/revolution, identical to the original 1927 conclusion of Vsekhsvyatskij.

Considering this body of work, one is led to concur with Whipple and Hamid (1972) that "the rate at which comets systematically change in brightness with age is not es-

³Vsekhsvyatskij (1958) still took the reverse viewpoint, now supposing the origin and replenishment of the comet reservoir from volcanic ejecta, mainly from the Jovian system. However, he seemed to favor a Venusian origin for 2P/Encke.

established satisfactorily on either an observational or a theoretical basis". There is little hope of clarifying the situation through attempts to homogenize the visible data. Aside from the perils of trying (or failing to try) to reduce an extremely inhomogeneous data set to a common photometric standard, the use of visible magnitudes to track activity is problematic. The degree to which visible brightness mirrors activity in the sense of mass loss is not clear and has been explicitly shown to vary in the case of 2P/Encke (A'Hearn and Millis, 1983; A'Hearn et al., 1984). Very little continuum is present in the spectrum of 2P/Encke except near aphelion where we presumably see the bare nucleus, and near-perihelion brightness at visible wavelengths is due primarily to emission from C₂, a relatively minor constituent with a mass fraction only 10⁻²-10⁻³ that of water (A'Hearn et al., 1984). For dusty comets, which do have reflected continua, extrapolation from visible brightness to mass loss rate depends critically on poorly understood factors such as the size distribution, scattering properties, and densities of the particles (A'Hearn et al., 1995). Thus, any extrapolation from visible magnitude to mass loss rate should be considered tenuous.

Even if one could reliably gauge total mass loss rates, the quantity more pertinent to the question of aging would be the mass loss rate of volatiles alone. When the volatiles are exhausted, the comet as such is essentially dead, regardless of the remnant mass. Since sublimation of volatiles drives virtually all cometary phenomena, the mass loss rate of volatiles is a natural index of activity, and one could define the characteristic activity level as the total mass of volatiles lost over a given orbit. A practical alternative is to directly compare mass loss rates of the dominant volatile at the same point on the orbit. The mass loss rate of water, the dominant volatile of 2P/Encke and probably of all comets at $r \lesssim 3$ AU, can be most reliably assessed through modeling of the strong near UV emission of OH, the primary product of H₂O photolysis. IUE has measured OH fluxes from 2P/Encke over 5 successive apparitions from 1980-1994, and IUE resident astronomers have routinely obtained calibration images of standard stars over the period. Recent work on chemical lifetimes in the coma allows us to quantify modeling uncertainties. Since IUE operations will cease after 1996, it is now appropriate to analyze the dataset for evidence of secular trends in activity.

3 Observations

We based our comparisons on OH fluxes in the near-UV electronic bands. The strong (0-0,1-1,1-0) bands of the OH (A ²Σ⁺ - X ²Π) electronic system occur in IUE's long wavelength region, centered at λ 3085, 3145, and 2827 Å, with relative band strengths of about (5-30):1:0.6. OH fluorescence efficiencies (*g*-factors) depend on the comet's heliocentric velocity (\dot{r}) through the Swings effect (Schleicher and A'Hearn 1988). While observed and theoretical band ratios agree reasonably well for most heliocentric velocities in a limited IUE dataset (Schleicher and A'Hearn 1988), we chose to compare only like bands in order to maintain the highest possible degree of uniformity.

2P/Encke observations were exclusively pre-perihelion at 3 apparitions (1980, 1990, 1993-94) and exclusively post-perihelion at 2 (1984, 1987). It is important not to mix the two types since asymmetry of activity about perihelion is well-documented for 2P/Encke, although it may be decreasing (Kamél 1991). To maximize S/N, OH abundance is usually derived from the strongest unsaturated band. It was not always possible, in this study,

to maintain this criterion along with those of uniform r and uniform band. While the dominant 0-0 band was suitable as the basis for our pre-perihelion comparison, the only pair of post-perihelion spectra obtained at comparable r included one (1984) saturated in 0-0. Thus we based post-perihelion results on the 1-0 band, even though the 1987 spectrum was well-exposed for 0-0 and therefore had rather poor S/N in 1-0. The 1-1 band, while stronger than 1-0, has lower S/N since it lies in a spectral region where IUE detector sensitivity is sharply decreasing.

9P/Tempel 1 observations were about 10 days post-perihelion both in 1983 and in 1994, 2 revolutions later.

The relevant observations are summarized in Table 1. We directly compared only observations made at nearly the same point in the orbit. Note, however, that this point is not uniquely defined since the orbits change slightly from one apparition to the next. One could use either r or ΔT or v as the criterion for comparable points, but they are not quite consistent. Note that the 1980 and 1983 spectra were obtained with the LWR camera while the later exposures used the LWP camera.⁴ The standard long-wavelength camera was switched in 1984 from the LWR to the LWP, and assessing the relative response of the two cameras is an important point in our analysis. All spectra were obtained through the large aperture (LWLA), nominally a $\sim 9.3'' \times 20''$ rectangle but actually slightly rounded at the ends. Only low-dispersion exposures centered on the nucleus were considered. For 2P/Encke, all exposures longer than 20 minutes were obtained in segments, returning either the comet or an offset star to a reference point between segments to check and update tracking. For 9P/Tempel 1, the 1983 spectrum was obtained in segments, while in 1994 we were able to expose continuously by guiding on a nearby star. Tracking errors in the 1990 2P/Encke images and in the 1994 9P/Tempel 1 image precluded accurate determination of OH 0-0 fluxes for these apparitions. We can, however, infer reasonable limits to systematic corrections of these fluxes.

4 Analysis

4.1 Extraction and Calibration

IUE low-dispersion data are delivered to the user in several forms, including an extracted spectrum. However, in order to account for irregularities in the background and in the positioning of the comet, we performed the spectral extractions ourselves, from the extended line-by-line (“ELBL”) data product of the IUE Spectral Image Processing System (IUESIPS). This is a spectral image in a format of 110 lines by approximately 900 pixels, pre-processed to correct for the geometrical distortion and photometric non-linearities characteristic of the analog SEC vidicon detectors, but not absolutely calibrated. The spectral sampling interval is $\sim 1.8 \text{ \AA}/\text{pixel}$ with an effective resolution of $\sim 11 \text{ \AA}$, while spatial sampling is $1.0785''/\text{line}$ with a nominal resolution of $\sim 3.75''$. Older spectra were reprocessed with the latest version of IUESIPS.

We employed our own library of IDL routines designed specifically for IUE data. All images were first dark-background subtracted by smoothing the background with a median filter to remove blemishes such as resseau (registration) marks and cosmic ray hits, and

⁴For details of IUE instrumentation and configuration, we refer the reader to Boggess et al. (1979)

then interpolating the smoothed background linearly across the exposed portion of the image, column-by column.

The 1993-94 images required special treatment. Comparison of 1980 and 1993 2P/Encke spectra (Figure 1a,b) shows a dramatic increase in continuum level. 2P/Encke in fact has no measurable UV continuum; the effect is due to physical degradation of the IUE satellite. This scattered light artifact of unknown origin, known by the somewhat ominous sounding name of “the streak”, first appeared in 1992 and had to be subtracted from all 1993-94 spectra. The severity of the streak is correlated with the β angle, which is basically the supplement of (180° minus) the solar elongation of the target. We removed the streak contribution by fitting each contaminated image to a composite of several archival blank sky images taken at approximately the same β , after dark background subtraction but before the spectral extraction. The streak images were registered according to pixel offsets determined from cross-correlation, then added. Because the streak has a strong spatial gradient across the slit, the fit was performed in two dimensions. After appropriate pixel offsets, a surface was fit to the ratio of comet pixel values to streak pixel values in wavelength bins where the cometary spectrum is presumed to have negligible flux. Since no UV continuum has ever been detected in 2P/Encke, its spectra served as a test of the method. A fit surface of the form $a_x x + a_y y + a_{xy} xy$ was essentially constant, and the residuals of the fit surface subtracted from the surface of ratios were uniform across the slit and normally distributed about zero, confirming both the validity of the method and the absence of reflected continuum. 9P/Tempel 1, on the other hand, does have real continuum, but a fit to a smaller region below 2800 Å gave good results. No improvement in residuals was gained from a quadratic fit. The streak image was multiplied by the fit surface and subtracted from the comet image. The resulting images appeared quite normal in both emission and continuum wavelength regions, and the extracted spectra were virtually indistinguishable from those derived from uncontaminated images, albeit with slightly lower S/N (Figure 1c).

We extracted each spectrum by integrating over the rectangular portion of the slit, a total of 14 lines or $15.1''$. If peak brightness was off-center, but clearly within the slit, fewer lines were used, centered on the photocenter.

We then converted arbitrary IUE flux units to physical fluxes, according to exposure time and a published inverse sensitivity function of wavelength for the respective camera. These functions, derived from standard star observations by IUE’s PHCAL program, refer to epoch 1978 for the LWR camera and to epoch 1985 or 1989 for the LWP.

Normally, correction for subsequent degradation of detector sensitivity with time, again using published formulae derived from PHCAL observations, completes the absolute calibration. Here, however, we deviated from the usual procedure. IUE absolute calibration is good to about $\pm 10\%$. Since our result in this study depends only upon the ratio of production rates, absolute calibration is irrelevant but accurate relative calibration, along with a legitimate statistical treatment of the associated uncertainties, is essential. In view of the length of our temporal baseline, the changes in detector sensitivity with time, and the change from the LWR to the LWP camera, we felt it necessary to fix the relative calibration more precisely than possible with the published formulae. We obtained sequences of archival images of HD60753 (spectral type B5), the primary PHCAL standard, spanning each relevant epoch. To account for pixel-to-pixel variation, we considered only exposures in which the star is trailed across the length of the aperture, simulating an extended source. Stellar and cometary spectra were extracted and calibrated, but with-

out applying the time correction. A linear fit with time to the brightness in the OH 0-0 bandpass was obtained for each calibration sequence, from which the relative responsivity at each cometary observation was read off. The standard deviation of each calibration was calculated from the scatter of the points about the best-fit line.

We then integrated over each pertinent emission line to find the total flux, and converted the integrated fluxes converted to brightnesses [B] in Rayleighs averaged over the area of the slit. Standard deviations in the line brightnesses were calculated from the scatter of points in adjacent baseline bins. A correction to the brightnesses due to a slight dependence of camera sensitivity on the head amplifier temperature (THDA) was applied (Imhoff 1986). This effect was as much as 3% for the LWR camera, but no more than 1% for the LWP.

4.2 Modeling

Water production rates ($Q_{\text{H}_2\text{O}}$) were derived by modeling the coma using the vectorial model developed by Festou (1981). Given an assumed production rate of a “parent” molecule (in this case H_2O), the model calculates the distribution in the coma of some “daughter” species (in this case OH) produced by dissociation. The parent is assumed to flow from the nucleus isotropically and with constant velocity. The model is obtained analytically, but differs from the widely used Haser model in that daughter velocities are assumed to be distributed isotropically in the parent’s rest frame rather than to be co-linear with the parent velocity. Along with the parent and daughter ejection velocities, model parameters include total water lifetime ($\tau_{\text{H}_2\text{O}}$), water lifetime against dissociation into OH (τ_{diss}), OH lifetime (τ_{OH}), and the angular dimensions of the field of view. Then, assuming emission by resonance fluorescence, one supplies the g -factor at 1 AU, allowing conversion of calculated column densities $N(\rho)$ into brightnesses $B(\rho)$, averaged over the specified field of view. It is assumed that g scales as r^{-2} , following theoretical results of Schleicher and A’Hearn (1988), from whom we take the values as well.

Since IUE’s field of view is small compared to the OH destruction scale length, the instrument sees only a fraction of the fluorescing molecules, so that the derived Q ’s are highly model dependent and modeling uncertainties account for most of the uncertainty in derived $Q_{\text{H}_2\text{O}}$ values. These errors have previously been difficult to quantify, but absolute results are probably uncertain by at least 25% and could easily be off by a factor of 2. However, since we are seeking only a relative answer for the same comet observed at the same point in the orbit, we can expect to do much better. Model-induced errors divide into two categories: (1) those resulting from erroneous model assumptions, and (2) those resulting from erroneous model parameters.

The most obvious erroneous assumption is that of spherical symmetry. Activity on most short period comets is probably dominated by discrete active areas covering only a small fraction of the surface area, as was shown to be the case for 1P/Halley (Keller et al., 1986). However, if coma morphology is relatively constant from apparition to apparition, then to a good approximation the ratio of the model answer to the correct answer at a given point in the orbit will be a constant, which will cancel out in the ratio of the Q ’s. This cancellation will be almost exact if the precise observing geometry is the same. 2P/Encke is well-suited to this type of analysis: its coma consistently has the form of a sunward cone or “fan” (Sekanina 1991) and it is in a near 3:10 resonance with the Earth, with observing geometry approximately repeating every 3 revolutions. Unfortunately, the

best geometrical match to the 1980 pre-perihelion observations was at the compromised 1990 apparition, but 1993 and 1980 observation dates differed by only 2 months and the fan-shaped coma was observed at both apparitions (Feldman et al. 1984, S. Larson private communication 1993). The post-perihelion apparitions, separated by only one revolution, were not as good a match. However, any deviation from spherical symmetry is much less in OH than in the carbon-based species mainly responsible for the asymmetrical visible brightness distribution, due both to the high lateral velocities attained by the parent H₂O molecules and to the long OH lifetime. In contrast to the striking asymmetry apparent in many images (Sekanina 1991), sunward and tailward OH brightness in 2P/Encke's 1980 apparition differed by a factor of only 1.6 (Feldman et al., 1984). As seen by IUE, any asymmetry should be even less, since its spatial axis is always oriented approximately 90° to the Sun-comet line. 9P/Tempel 1 is almost exactly in a 2:11 resonance at the current epoch, and the geometrical match was nearly perfect.

The most uncertain parameters in the model are the H₂O outflow velocity and the lifetimes. The outflow velocity, while poorly known, should be a function only of the particular comet and of r , and so should be constant within each comparison. Therefore, since the model is approximately linear in the outflow velocity for a field of view which is small compared to H₂O and OH destruction scale lengths, the velocity will cancel out in any such ratio, independent of the observing geometry. Lifetimes, on the other hand, are intrinsically variable and thus do not necessarily cancel out of the model ratios even if the geometries are identical. The variability arises because H₂O and OH destruction cross-sections are appreciable only in the region below $\sim 1860 \text{ \AA}$, where the solar flux is highly variable on the ~ 11 year time scale of solar activity cycles and moderately variable on the ~ 1 month time scale of solar rotation (Budzien et al. 1994). This dependence on solar activity has been recognized for at least the last 15 years as a major source of uncertainty in the interpretation of cometary UV emissions (Oppenheimer and Downey 1980). Assuming any errors from the imperfect geometrical match to be no larger than 2nd order effects, then to 1st order the model uncertainties for this work reduce to uncertainties in the lifetimes.

Although Cochran and Schleicher (1993) attempted to empirically constrain lifetimes for a variety of solar conditions by finding best parameter space fits of observed OH spatial profiles to vectorial model results, there are too many free parameters to find a unique fit. However, H₂O destruction mechanisms are well-understood and cross sections have been measured in the laboratory. Therefore, all relevant destruction rates can be reliably calculated if one can obtain the solar spectrum at $\lambda < 1860 \text{ \AA}$ and the solar wind flux for the date in question. While the UV photon fluxes are only sporadically measured, they are correlated with solar indices which are measured on a nearly daily basis. Much previous modeling has used theoretically derived lifetimes following the approach of Crovisier (1989), who calculated photolysis rates for two solar spectra, one chosen to represent the quiet and one the active Sun, then linearly interpolated between the maximum and minimum rates according to one of the measured indices, the 10.7-cm radio flux. We know of no attempts to statistically assess the uncertainty of such results.

We adopt for this work a more rigorous approach by Budzien (1992) and Budzien et al. (1994), who use the observed correlations of measured indices with flux in individual wavelength bins to synthesize a solar spectrum for the particular observation date. The 10.7-cm flux and its average over 3 solar rotations (~ 81 days) correlate fairly well with extreme ultraviolet ($\lambda < 1000 \text{ \AA}$) fluxes, but for far ultraviolet ($1000 < \lambda < 2000 \text{ \AA}$) the

preferred index is the equivalent width of the He line at 10830 Å [He₁₀₈₃₀], for which a much tighter correlation is observed. Total Lyman- α flux, responsible for about 40% total H₂O destruction rates, correlates with He₁₀₈₃₀ to within 5%, and linear fits in each 1 nm FUV bin from 125-195 nm, which together account for about 50%, have standard deviations of less than 10%. The synthetic spectrum, solar wind ion flux, and measured cross sections, and their uncertainties, are then used to generate H₂O and OH photolysis rates and their uncertainties. The OH destruction rate includes a contribution, dependent on \dot{r} via the Swings effect, from predissociation during resonance fluorescence, for which we use values from Schleicher and A'Hearn (1988).

For this work, we specialized the error propagation in the lifetimes to the case where one seeks only a ratio of Q 's. Since IUE's field of view is small compared to the destruction scale length of OH, the derived Q is largely insensitive to τ_{OH} . Since the field is also small compared to the destruction scale length of H₂O, the derived Q depends only weakly on the total H₂O lifetime but scales to τ_{diss} . Thus, to a good approximation, the ratio of Q 's depends only on the ratio of the τ_{diss} 's, with the same relative uncertainty. We therefore neglected uncertainties in the absolute calibration of the solar fluxes and in the dissociation cross sections, since these uncertainties are systematic in nature and to first order will scale out in the ratio of τ 's.

One must take care to generate the solar spectrum as seen at the comet and not at the Earth. Most of the dissociating flux comes from discrete active areas on the Sun, and so varies with solar latitude and longitude, while the relevant solar indices and the solar wind flux are measured from Earth or Earth orbit. Day-to-day variation in the UV flux results primarily from the distribution of active regions on the surface of the Sun rather than from intrinsic variability of the regions, so one may estimate the flux seen by the comet if the times at which the solar indices are measured at the Earth are adjusted by the interval in which the Sun rotates through the difference in heliographic longitude of the Earth and the comet. We made no attempt to account for differences in latitude because both 2P/Encke and 9P/Tempel 1 have low-inclination orbits and Earth-comet heliographic latitude differences were only (5-15) $^\circ$.

Estimating the solar wind flux is far less certain due to intrinsic variability, but solar wind accounts for only about 10% of the total destruction rates and has no effect on the production of OH, so for the small aperture even large uncertainties will have only minimal effect on the results. Latitudinal variations measured by *Vela 3* and *Vela 4* spacecraft were no more than 30% over a 14 $^\circ$ wide equatorial region (Brandt et al. 1973), much less than the intrinsic uncertainty.

While our comparison is not very sensitive to the parent velocity v_p or daughter velocity v_d used, we adopt $v_p \sim 0.85r^{-.5}$ km/s, based on measured coma velocities at the 1986 1P/Halley Giotto encounter and on several theoretical and empirical studies (Budzien et al. 1994). We use $v_d=1.05$ km/s, from Budzien's theoretical calculations.

4.3 Correcting for Tracking Errors: 2P/Encke

Spatial profiles for each of the two 1990 images for which OH 0-0 was unsaturated indicate that the photocenter was at or beyond the edge of the slit, consistent with offsets produced by tracking errors. While this precluded obtaining precise results for these spectra, we were able to deduce the most probable offsets by comparing the observed profiles with model spatial profiles, and derived approximate correction factors from these offsets. Both

exposures were obtained in segments, and the comet was positioned at the start of each segment by offsetting it from a reference point on IUE's Fine Error Sensor (FES). The reverse maneuver followed each segment, and the residual offset of the comet from the reference point gave a formal tracking error. This formal error reflects any errors in maneuvering and in locating the photopoint as well as genuine tracking errors. For LWP 18881, the average formal tracking error after 2 segments was about $6''$. For LWP 18833, the formal error was $20''$ for the first of 4 segments but unknown for the rest, because the FES was unable to accurately lock up on the comet. To estimate the actual offsets, we used the vectorial model to generate brightness profiles for a hypothetical $9.3'' \times 3.75''$ aperture, corresponding to the nominal resolution, and then slid plots of $\log(B_{\text{obs}})$ along plots of $\log(B_{\text{model}})$ to estimate the range of distances where the slopes matched (Figure 2b,c). We then read off from the model profiles the corresponding limits for Q . We take the reasonably good match (Figure 2a) of a similar model to a composite of 1980 offset exposures as a validation of this approach. We found offsets of $(25 \pm 10)''$ for LWP 18833 and $(10 \pm 5)''$ for LWP 18881.

4.4 Correcting for Tracking Errors: 9P/Tempel 1

The 1994 9P/Tempel 1 image was obtained as a single 4-hour exposure, by priming the FES to check the offset of the guide star from the LWLA at 5 minute intervals, and locking the star to calculated coordinates if the error was more than about $1''$. Although the net formal tracking error was negligible, the spatial profile was unusual, with peaks at both edges of the slit. However, the spectrum was clearly not saturated, as raw image DN (data number) levels were only about 120, half of the maximum 255. Since the guidestar was moving into the streak during the exposure, we suspect that the high background gradient was confusing the FES. Where the background gradient is strong, the apparent peak of a superimposed point spread function (PSF) will be shifted. We used the observed background counts to estimate the maximum offset that might result from this effect. The star was moving at about 60° with respect to the spatial axis of the slit, so the gradient along the slit was about $2\times$ the observed gradient along the path. From FES images of stars, the observed FWHM of the point spread function is about $(10 - 15)''$. To derive a generous upper limit on the plausible offset, we multiplied the plot of counts along the path by 4 instead of 2 and superimposed the PSF Gaussian. The resulting offset was $(3 - 4)''$. To be conservative, we assume a maximum plausible offset of $7.5''$, placing the comet just at the edge of the extraction slit.

5 Results

5.1 Modeling Errors

In order to assess separately the contribution of each source of uncertainty in the model, we varied each independent lifetime by one standard deviation while holding the others fixed. Since the model parameters $\tau_{\text{H}_2\text{O}}$ and τ_{diss} are not independent, we varied $\tau_{\text{H}_2\text{O}}$ by only the uncertainties from photoionization and solar wind rates when holding τ_{diss} fixed, and varied $\tau_{\text{H}_2\text{O}}$ as well as τ_{diss} according to the uncertainty due to photodissociation while holding ionization and solar wind destruction rates fixed. While, as expected, derived Q 's

approximately scaled to τ_{diss} and were quite insensitive to independent changes in the other lifetimes, we included all uncertainties in our analysis. Theoretical uncertainties plus uncertainties in the measured solar indices, primarily He_{10830} , resulted in errors of less than 7% in τ_{diss} . Combined uncertainties, including solar wind uncertainties of 50-80%, produced errors of order 10% in $\tau_{\text{H}_2\text{O}}$ and 12-15% in τ_{OH} , and each contribution propagated to an error of 1.5-2% in the model. Therefore, the error budget for each model scale factor, M , is

$$\begin{aligned} \left(\frac{\sigma_M}{M}\right)^2 &= \left(\frac{\sigma_{\tau_{\text{diss}}}}{\tau_{\text{diss}}}\right)^2 + \left(\frac{\sigma_M[\text{H}_2\text{O ionization, SW destruction}]}{M}\right)^2 + \left(\frac{\sigma_M[\tau_{\text{OH}}]}{M}\right)^2 \\ &= (.07)^2 + (.02)^2 + (.02)^2 \approx (0.075)^2. \end{aligned}$$

5.2 2P/Encke

Uncertainties

RMS errors in flux were $< 1\%$ in 1980 and $\sim 1.5\%$ in 1993, and calibration sequence uncertainties about 6% and 3%, respectively. Combining these with the 7.5% uncertainty σ_M/M gives total uncertainty σ_Q/Q of about 10% and 8.5%, respectively, for the two apparitions. Thus the statistical uncertainty in the pre-perihelion ratio Q_{93}/Q_{80} is about 13%.

RMS errors in flux were $< 1\%$ in 1984 and $\sim 5\%$ in 1987, and calibration sequence uncertainties were about 3%, giving combined uncertainties σ_Q/Q of about 8% and 9.5%, respectively. Thus the statistical uncertainty in the post-perihelion ratio Q_{87}/Q_{84} is about 12.5%.

The probable angular offsets for the 1990 spectra represent projected distances of (15000 ± 6000) km for LWP 18833 and (6000 ± 3000) km for LWP 18881. From the vectorial model profiles, we read off corresponding flux correction factors of 2.1 ± 0.5 and 1.4 ± 0.3 , giving total errors in derived Q 's of 25% and 22%, respectively.

Production Rates

Derived water production rates, with error bars, are plotted in Figure 3, and results are summarized in Table 2. All values have been normalized to the 1993-94 calibration sequence.

Based on the 1980 and 1993 spectra closest in r , LWR 09135 and LWP 27121, we derive the result

$$Q_{93}/Q_{80} = 0.85 \pm 0.11$$

for the pre-perihelion change in activity of 2P/Encke over 4 revolutions, equivalent to an average decline of about (-4.0% or 0.044 magnitude)/revolution. Thus our 3- σ upper limit on pre-perihelion change over 4 revolutions is 33%, or (9.5% or 0.11 magnitude)/revolution.

Comparing the 1984 and 1987 spectra, we derive the formal result

$$Q_{87}/Q_{84} = 1.16 \pm 0.14$$

for the post-perihelion change in activity over a single revolution, an increase equivalent to about -0.16 magnitudes. This should be considered a lower limit, since the 1987 observation was at somewhat greater r . A power law exponent of 3.5-4, characteristic of the 1980 apparition (Feldman et al. 1984) would increase the ratio by about 5%, to ~ 1.22 . Our $3\text{-}\sigma$ upper limit on post-perihelion change is (42% or 0.38 magnitude)/revolution.

5.3 9P/Tempel 1

Uncertainties

RMS errors in flux were about 6% in 1983 and 5% in 1994, calibration sequence uncertainties about 2% for each, and combined uncertainties σ_Q/Q about 10% and 9%, respectively. The maximum plausible angular offset of 7.5° for the 1994 spectrum represents a projected distance of 5000 km, corresponding to a correction factor of 1.15 according to the vectorial model profile.

Production Rates

The results are included in Table 2 and Figure 3. 9P/Tempel 1 appears to have faded by about 50% over two revolutions. Allowing for the maximum plausible systematic error, we derive an upper limit of

$$Q_{94}/Q_{83} \leq 0.51 \pm 0.07$$

for the change in activity of 9P/Tempel 1 over two revolutions, equivalent to an average decline of about (29% or 0.37 magnitude)/revolution. Our $3\text{-}\sigma$ lower limit to the fading is 28%, or (15% or 0.18 magnitude)/revolution. We do not, however, feel as confident of this conclusion as of that for 2P/Encke. While we believe that we have been generous in our estimate of a possible systematic effect due to pointing errors, we do not completely understand the anomaly in the 1994 spectrum. One must necessarily attach a caution flag to any such result.

6 Discussion

The results for the two comets are strikingly different. The results for the pre- and post perihelion phases of 2P/Encke's orbit also differ, but the difference is of marginal statistical significance. Before considering possible inferences, we must mention certain caveats:

- 1) When comparing only single observations, it is necessary to rule out rotationally modulated variation as an explanation for any observed differences. They are unlikely in the case of 2P/Encke, since our search of the literature revealed no reported evidence of variability on a time scale of hours or days. This is probably a consequence of the orientation of the poles. 2P/Encke's coma typically has the form of a relatively narrow cone or "fan", which Sekanina (1988) has modeled as highly collimated flow from a discrete, high-latitude, source. He further concludes that the pole must lie nearly in the orbital plane and point approximately toward the Sun. Thus, insolation to the active area would

be relatively constant through any rotation. We can not rule out such an explanation for the case of 9P/Tempel 1, but neither are we aware of any data suggesting short-term variability.

2) The light curve may change from one apparition to the next. In fact, the time of 2P/Encke's peak visible brightness is slowly shifting from pre- to post-perihelion. Kamél (1991) has shown that all of the apparent fading reported by Kresák and Kresáková and others can be explained by this effect, since their dataset is biased towards observations clustered around the point in the orbit at which the peak was located in the late 19th century. Our results are consistent with a similar trend in the water production curve of 2P/Encke.

3) We have less confidence in our post-perihelion 2P/Encke results than we do in our pre-perihelion results, because of the poor geometrical match in post-perihelion observing geometries. While, as mentioned in the discussion of modeling, the effect should be rather small, we cannot rule it out as an explanation for the post-perihelion results.

At the $2\text{-}\sigma$ confidence level, our results for 2P/Encke are consistent with either an increase or a decrease in activity, both pre- and post-perihelion. At the $1\text{-}\sigma$ confidence level, however, our 2P/Encke results are consistent with an average drop in $Q_{\text{H}_2\text{O}}$ of (1-7)%/revolution pre-perihelion, but are not consistent with any increase. The post-perihelion results, on the other hand, are consistent with an increase of (2-30)%/revolution but are not consistent with any decrease. While our pre-perihelion result is nearly identical to the fading rate quoted by Kresák and Kresáková, we are skeptical that either result is statistically significant. It is interesting to note, however, that our results are consistent with the reported shift of the visible lightcurve towards post-perihelion, and that the magnitude of our pre-perihelion result is very close to the center of the range given by Kamél (1991) for apparent visible fading due to this effect. Data are too sparse to allow an estimate of the magnitude of a corresponding post-perihelion effect. However, the disparity in the magnitudes of our pre- and post-perihelion results suggests that real physical evolution, as opposed to a simple precession of 2P/Encke's pole, may be responsible for the shifting lightcurve. If, as Sekanina (1991) supposes, the activity on 2P/Encke is confined to two discrete sources, an older, declining source active primarily pre-perihelion and a recently activated post-perihelion source, then our results may be diagnostic of the evolution of distinct active areas.

With high eccentricity, small perihelion distance, and aphelion well inside the orbit of Jupiter, 2P/Encke is on an unusually stable orbit which resembles more those of Earth-crossing asteroids than of typical Jupiter-family comets. 9P/Tempel 1, on the other hand, has a more erratic orbital history. Currently close to the 2:1 resonance with Jupiter, the comet was lost for 13 perihelion passages between 1879 and 1966 during which time the orbital elements apparently evolved considerably due to Jovian encounters. Kresák (1991) identified this comet as one with moderate but erratic brightness variations superimposed on essentially stable long-term behavior. It is reasonable to suspect that the character of a comet's long-term brightness variations is related to its orbital history, but one can only speculate on the nature of such a relationship. Two factors which may be likely to influence the pattern of evolution of activity are the comet's physical age itself, and close planetary encounters.

Because of its small perihelion distance and its frequency of perihelia, there is a tendency to think of 2P/Encke as the most physically aged comet - it "may well be the Methuselah of comets" (Whipple 1985). While the chaotic nature of most short-period orbits (Levison and Duncan 1994) makes it impossible to use dynamical arguments to compare physical ages, there are reasonable grounds to suppose that 2P/Encke may be considerably older than 9P/Tempel 1. With five times more distant a perihelion and nearly twice as long a period, 9P/Tempel 1 currently receives considerably less average insolation and peak insolation than does 2P/Encke. To be comparable to 2P/Encke in physical age, 9P/Tempel 1 would have had to have evolved to its current orbit from an Encke-like orbit. But according to the integrations of Valsecchi et al. (1995), Encke-like orbits have a greater than 50% probability of falling into the Sun. One would expect the majority of the remainder to be ejected from the solar system rather than to be captured into a near resonance with Jupiter. If 2P/Encke is much older than 9P/Tempel 1, then the difference in the character of their brightness variations is consistent with the supposition that gradual mantle build-up is an important evolutionary mechanism for short-period comets. Then newer short-period comets would have not only a larger active surface, but would be likely to have a larger number of discrete active regions. If an individual active area is characterized by gradual evolution, but with a certain probability of a discrete event such as the collapse or eruption of a vent, then the probability of observing one such event would become greater as the number of individual sources becomes larger. The observed amplitude of such an event would, however, be moderated by the background activity of the other sources. Thus activity on newer short-period comets may be characterized by fairly erratic evolution. It may also be that close encounters with Jupiter can induce erratic activity patterns through the effects of tidal stresses on the surfaces or interiors of comets.

While the current baseline is too short to permit any conclusions about genuine trends, our results offer the hope that real answers may begin to emerge with only a modest extension of the baseline. Unfortunately, prospects for such an extension appear somewhat doubtful. When IUE is turned off in late 1996, HST will be the only spacebased instrument capable of obtaining these kinds of data, and its lifetime is unlikely to dramatically exceed that of IUE. The OH 3085 Å transition is accessible to high-altitude, ground-based, narrow-band photometry, which has already yielded H₂O production rates for many comets (A'Hearn et al. 1995). Such an approach has both advantages and disadvantages when compared to spaced based spectrophotometry. A wider sampling of the light curve is likely to be possible from the ground, and the large field of view used means that derived values of Q will be less model dependent, since the telescope will see more of the coma. Observing geometry, $\tau_{\text{H}_2\text{O}}$, τ_{diss} , and parent and daughter velocities become largely irrelevant. However, the result now scales with τ_{OH} , which is less well-determined than τ_{diss} and which depends on the highly uncertain solar wind flux, particularly in the outer coma. We calculated the effect of varying solar wind flux on vectorial model results for both IUE's $9.3^{\circ} \times 15.1^{\circ}$ aperture and one 150° in diameter, within the range used with imaging photometers. Near-Earth solar wind flux, from IMP8 spacecraft data, can vary by up to a factor of 100, from $(0.4-40) \times 10^8$ ions/cm²/sec. For the mean flux over 1993-94, $(4 \pm 3) \times 10^8$, the corresponding uncertainty in Q was nearly 15% for the large field of view but $< 7\%$ for the IUE field. Further, many comets, including 2P/Encke, are typically observed near twilight with the attendant high air masses and extinction coefficients, so that calibration and RMS uncertainties in flux can be appreciably higher

than from space, and one must guard against contamination from background stars. This type of observation is capable of answering the secular variation question, but probably only over a much longer baseline than is possible with the present approach, at least for comets for which geometry repeats fairly frequently.

7 Conclusion

We have shown that by selecting observations with comparable geometry from well-calibrated datasets of spacebased spectrophotometry and modeling them appropriately, one is able to constrain relative activity levels over far shorter baselines than was previously possible. The method is primarily applicable to comets occupying relatively short-term resonances with the Earth's orbit.

We have shown that a rapid secular fading of 2P/Encke, the comet aging most rapidly in a chronological sense, which others have deduced from visible magnitude data, is not supported by mass loss rates derived from IUE observations of OH emission over 5 apparitions from 1980-1994. In seeking relative abundances of other volatiles to water, one can confidently compare data from pre-perihelion observations over timescales of a few apparitions with uncertainties of $\leq 10\text{-}20\%$. Post-perihelion behavior may be changing more rapidly, and the discrepancy between the two behaviors may reflect the existence of two distinct active areas.

We found that 9P/Tempel 1 may have faded by a factor of 2 over just 2 revolutions between 1983-1994. Although systematic error was clearly present, a reasonable and probably generous correction suggested that the decline was indeed real, and that that the comet faded by at least 28% over the interval, at the $3\text{-}\sigma$ confidence level.

An important goal of cometary astronomy is classify observed attributes, such as relative abundances, according to whether they are primordial or represent evolutionary effects. It is therefore necessary to have some means of assigning physical ages to comets. To date, the physical ages of comets can be assessed only in a statistical sense. We speculate that the character of long-term brightness variations might be diagnostic of the active surface fraction, and therefore of the physical age, of comets. Since detailed information about the surfaces of cometary nuclei and the number, character, and morphology of sources of activity is necessarily inaccessible from the near-Earth environment, this can be tested only by in-situ studies.

The time interval spanned by our data is too short to permit firm conclusions about long-term behavior. However, our criterion of selecting only observations at comparable geometry and our adaptation of recent work on photochemical lifetimes to the calculation of relative activity levels has reduced modeling uncertainties to the point where an extension of the current baseline by only a few apparitions could yield important knowledge. However, it might be some time before an extension at the present level of precision becomes possible. While ground-based high altitude observations hold promise of meaningful long-term monitoring of OH fluxes, the difficulties of observing through the Earth's atmosphere and of constraining OH lifetimes tend to limit the precision with which these data can be compared. IUE will not observe 2P/Encke, 9P/Tempel 1, or any other known short-period comet again. The potential of HST to augment the present database is substantial, but demands on observing time make full realization of this potential problematic. Investment in a small, dedicated comet survey telescope is necessary

if we are to fully reap the potential of comets to advance our understanding of the solar system.

A new imaging spectrometer is scheduled to be installed on HST in 1997, the year of 2P/Encke's next return, and we believe that observing 2P/Encke should be given a high priority at every accessible apparition for which the new instrument is operational. HST should be used to extend the UV database of other short-period comets in near resonance with Earth, and to obtain concurrent cometary observations with any new UV spacecraft. By such cross-calibration, we might begin to build up a truly homogeneous dataset on cometary H₂O which could serve as a crucial reference for other cometary studies. Since spacecraft have limited lifetimes, such a "leapfrog" approach may be the only way to maintain a uniformly calibrated spacebased dataset.

We note also that 46P/Wirtanen ($P \sim 5.5$ yr), the target of the Rosetta mission rendezvous in 2013, is currently in a 2:11 resonance with the Earth, and could be accessible to HST in both 1997 and 2008, when the geometry repeats. Combined with knowledge about the evolution of this comet's activity, the Rosetta mission could indeed provide the first piece of the key whereby we might begin to decipher the code of long-term variations of activity.

Acknowledgements

NASA's IUE project and ADAP supported this work through several grants, the last of which were NAG5-2093 and NAG5-1272, respectively. We would like to thank the many people at IUE who assisted in obtaining the data, including Jim Caplinger, Mike Carini, Don Luttermoser, Charles Profitt, Scott Snell, and Tom Walker, all of whom were instrumental in the 1993-94 observations. Scott Snell also provided tracking data for the 1994 9P/Tempel 1 spectrum and assisted in interpreting them. We acknowledge as well the help of the staff at the IUE Data Analysis Center (IUEDAC), notably Randy Thompson, in reducing the data and in locating appropriate sky background and stellar calibration images. We are also grateful to the staff at NASA's Data Archive and Distribution Service (NDADS), including Michael Van Steenberg and Winny Davenport, for help in retrieving archival images.

References

- A'Hearn, M.F., R.L. Millis, and D.T. Thompson, The Disappearance of OH from Comet Encke. *Icarus*, **55**, 250-258, 1983.
- A'Hearn, M.F., P.V. Birch et al., Comet Encke: Gas Production and Light Curve, *Icarus*, **64**, 1-10, 1985.
- A'Hearn, M.F., R.L. Millis, et al., The Ensemble Properties of Comets: Results from Narrowband Photometry of 85 Comets, 1976-1992. *Icarus* **118**, 223-270, 1995.
- Bobrovnikoff, N.T., Investigations of the Brightness of Comets, Part I. *Contr. Perkins Obs.*, **15**, 1941.
- Bobrovnikoff, N.T., Investigations of the Brightness of Comets, Part II. *Contr. Perkins Obs.*, **16**, 1942.
- Brandt, J.C., R.S. Harrington, and R.G. Roosen, Interplanetary Gas. XIX. Observational Evidence for a Meriodional Solar-Wind Flow Diverging From the Plane of the Solar Equator. *Astrophys.J.*, **184**, 27-31, 1973.
- Boggess, A., F.A. Carr, D.C. Evans. et al., The IUE Spacecraft and Instrumentation. *Nature*, **275**, 372-377, 1978.
- Budzien, S.A., *Physical and Chemical Processes of the Inner Coma Observed in Mid-ultraviolet Cometary Spectra*. Ph.D. Thesis, Johns Hopkins University, 1992.
- Budzien, S.A., P.D. Feldman, and M. Festou, Solar Flux Variability and Lifetimes of Cometary H₂O and OH. *Icarus*, **107**, 164-188, 1994.
- Cochran, A.L., and D.G. Schleicher, Observational Constraints on the Lifetime of Cometary H₂O. *Icarus*, **105**, 235-253, 1993.

- Crovisier, J., The Photodissociation of Water in Cometary Atmospheres. *Astron. Astrophys.*, **213**, 459-464, 1989.
- Feldman, P.D., H.A. Weaver, and M.C. Festou, The UV Spectrum of Periodic Comet Encke (1980 XI). *Icarus*, **60**, 449-463, 1984.
- Ferrin, L., and C. Gil, The Aging of Comets Halley and Encke. *Astron. Astrophys.*, **194**, 288-296 1988
- Festou, M.C., The Density Distribution of Neutral Compounds in Cometary Atmospheres. *Astron. Astrophys.*, **95**, 69-79, 1981.
- Imhoff, C.L., Correcting IUE Fluxes for Temperature Effects, *IUE NASA Newsletter #31*, p.11-12, 1986.
- Kamél, L., The Evolution of P/Encke's Light Curve: No Secular Fading, a Vanishing Perihelion Asymmetry. *Icarus*, **93**, 226-245, 1991.
- Koslov, W., On the Brightness of Encke's Comet. *Russian Astr. Jour.*, **6**, 81-83, 1929.
- Kresák, L., The Aging and Brighness Decrease of Comets. *Bulletin of the Astronomical Institute of Czechoslovakia*, **25**, 87-112, 1974.
- Kresák, L., and Kresáková, Absolute Brightness Variations in Periodic Comets, Part I. *Bulletin of the Astronomical Institute of Czechoslovakia*, **40**, 269-284, 1989.
- Kresák, L. and Kresáková, Absolute Brightness Variations in Periodic Comets, Part II. *Bulletin of the Astronomical Institute of Czechoslovakia*, **41**, 1-17, 1990.
- Levison, H.F., and M.J. Duncan, The Long-Dynamical Behavior of Short-Period Comets. *Icarus*, **108**, 18-36, 1994.
- Marsden, B.G., One Hundred Periodic Comets. *Science* **155**, 1207-1213, 1967.

Marsden, B.G., Comets and Nongravitational Forces. *Astron. J.*, **73**, 367-379, 1968.

Schleicher, D.G., and M.F. A'Hearn, The Fluorescence of Cometary OH. *Astrophys. J.*, **331**, 1058-1077, 1988.

Sekanina, Z., Secular Variations in the Absolute Brightness of Short-Period Comets. *Bulletin of the Astronomical Institute of Czechoslovakia*, **15**, 1-7, 1964.

Sekanina, Z., A Model for the Nucleus of Encke's Comet. In *The Motion, Evolution of Orbits, and Origin of Comets*, IAU Symposium 45, ed. G.A. Chebotarev, E.I. Kazimirchak-Poloskaya, B.G. Marsden (D. Reidel: Dordrecht), 1972, pp. 301-307.

Sekanina, Z., Outgassing Asymmetry of Periodic Comet Encke. I. Appearances 1824-1984. *Astron. J.*, **95**, 911-924, 1988.

Sekanina, Z., Encke, the Comet. *Jour. RAS Canada*, **85**, 324-376, 1991.

Valsecchi, G.B. et al., The Dynamics of Objects in Orbits Resembling That of P/Encke, *Icarus*, **118**, 169-180, 1995.

Vsekhsvyatskij, S., The Brightness of Comet Encke. *Russian Astr. Jour.*, **4**, 298-301, 1927.

Vsekhsvyatskij, S., On the Decrease of the Brightness of Comet Encke. *Russian Astr. Jour.*, **6**, 84-87, 1929.

Vsekhsvyatskij, S., On the Disintegration of Short-Period Comets. *MNRAS*, **90**, 706-721, 1930.

Vsekhsvyatskij, S., *Physical Characteristics of Comets* (English Translation), Israel Program for Scientific Translations, published for NASA and NSF, original 1958.

Whipple, F.L., A Comet Model. I. The Acceleration of Comet Encke. *Astrophys.J.*, **111**, 375-394, 1950.

Whipple, F.L., Brightness Changes in Periodic Comets. *Astron. J.*, **69**, 152, 1964.

Whipple, F.L. and D.H. Douglas-Hamilton, Brightness Changes in Periodic Comets. *Mém. Soc. Roy. Sci. Liège*, **12**, 469-480, 1966.

Whipple, F.L. and S.E. Hamid, A Search for Encke's Comet in Ancient Chinese Records, a Progress Report. In *The Motion, Evolution of Orbits, and Origin of Comets*, IAU Symposium 45, ed. G.A. Chebotarev, E.I. Kazimirchak-Pooskaya, B.G. Marsden (D. Reidel: Dordrecht), 1972, pp. 152-153.

Whipple, F.L., *The Mystery of Comets* (Smithsonian Institution Press: Washington, D.C.), 1985, p.101.

Figure Captions

Figure 1. Reduced IUE 2P/Encke spectra from 1980 and 1993. In a.), the 1980 spectrum has no measurable continuum. In b.), the 1993 spectrum shows contamination by the “streak” artifact. The result of subtracting a composite of blank-sky images to remove the streak is shown in c.).

Figure 2. Estimating probable pointing errors for 1990 pre-perihelion 2P/Encke spectra. In a.), the symbols represent the actual spatial profile from 4 LWR images offset along IUE’s x-axis, which lies approximately along the spatial axis of the slit; the curve is the spatial profile calculated by the vectorial model for those observations, using a $\sim 9.3^{\hat{n}} \times 3.75^{\hat{n}}$ slit. The latter dimension is IUE’s nominal spatial resolution. In b.) and c.), actual and model profiles are shown for LWP 18833 and LWP 18881, the 1990 spectra with uncertain offsets. We estimated the offsets by sliding the actual profile along the model profile until the fit was optimized. We then took the position of the center of the actual profile (solid lines) as the most probable offset. The dashed lines represent our estimates of the uncertainty in the position of the best fit. The slight asymmetry in the OH coma, evident in a.), suggests that the estimated uncertainties are probably too low.

Figure 3. Derived water production rates for 2P/Encke and 9P/Tempel 1. The 1990 2P/Encke points have been corrected upward for pointing errors, and their error bars include uncertainties in the correction. The 1994 9P/Tempel 1 point has not been corrected for pointing error, but the asymmetrical error bar reflects the range of plausible corrections.

Figure 1 - 2P/Encke IUE Spectra 1980, 1993

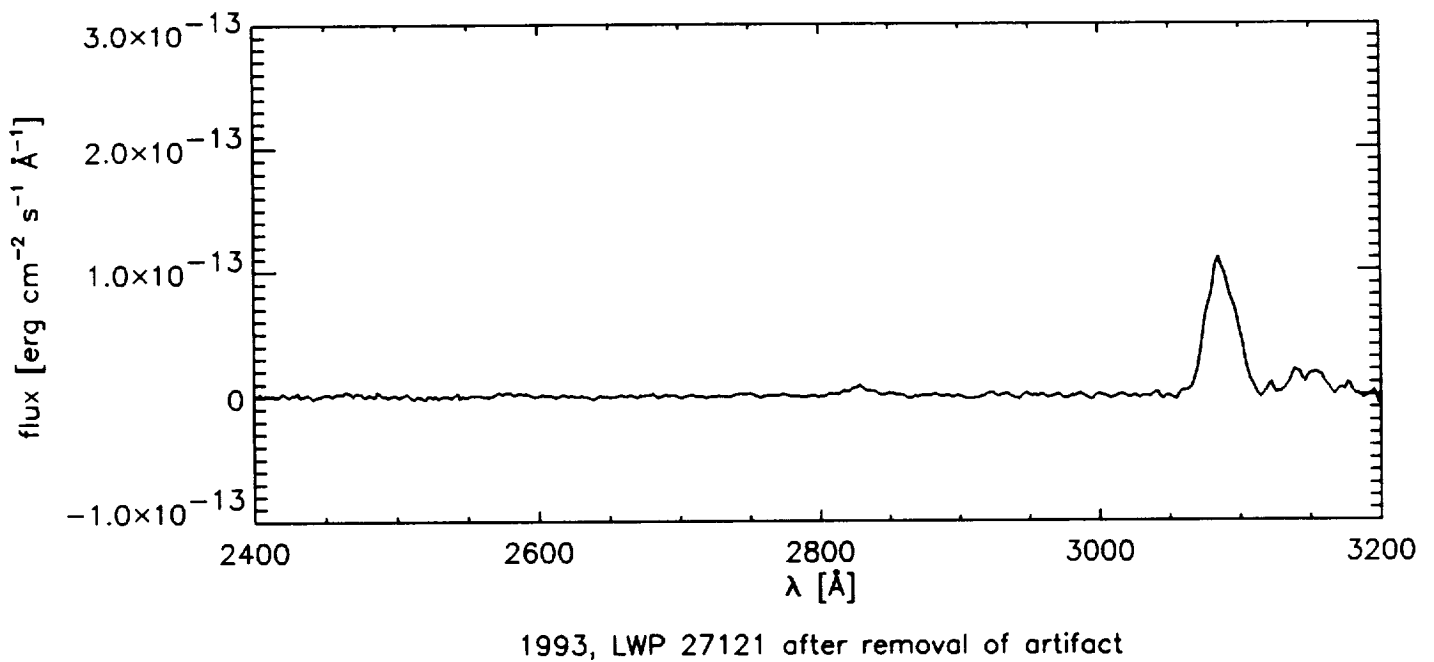
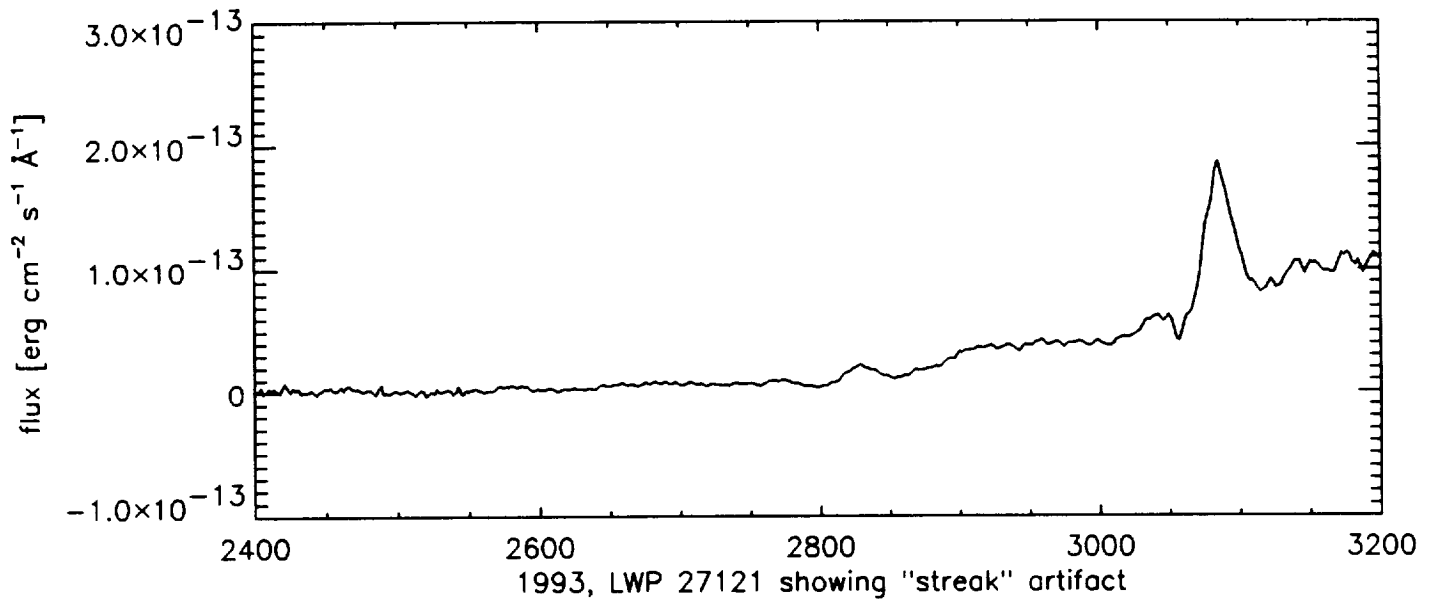
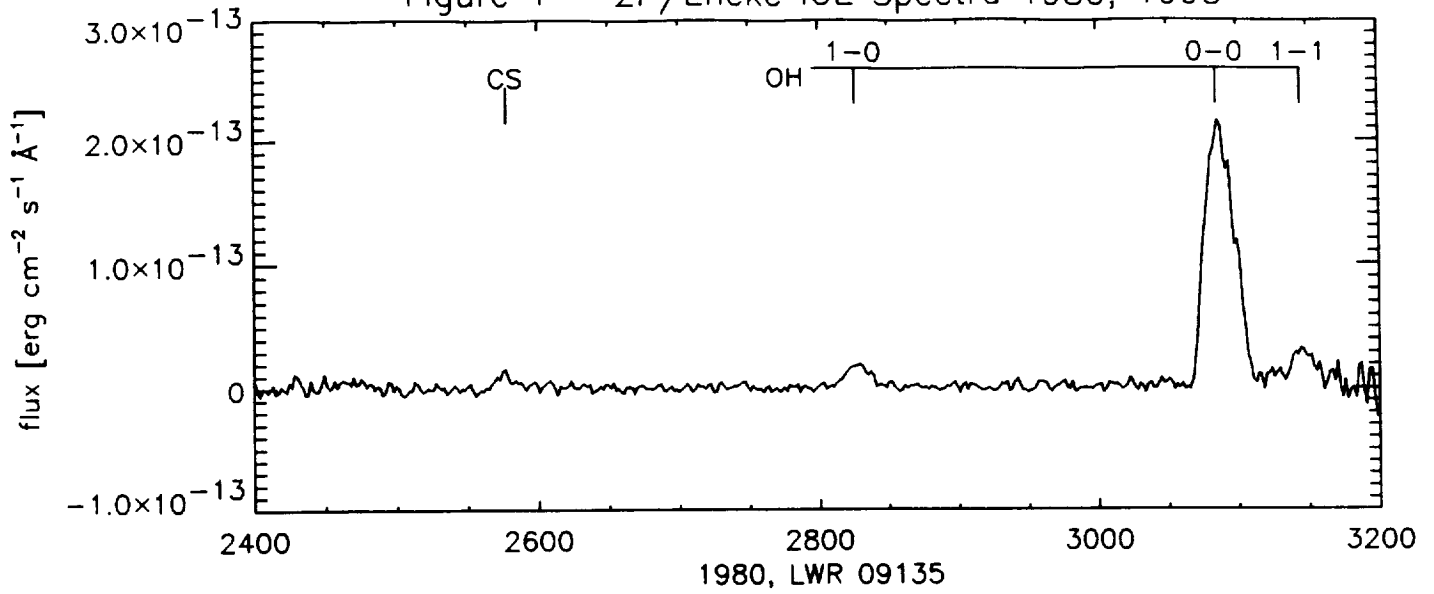
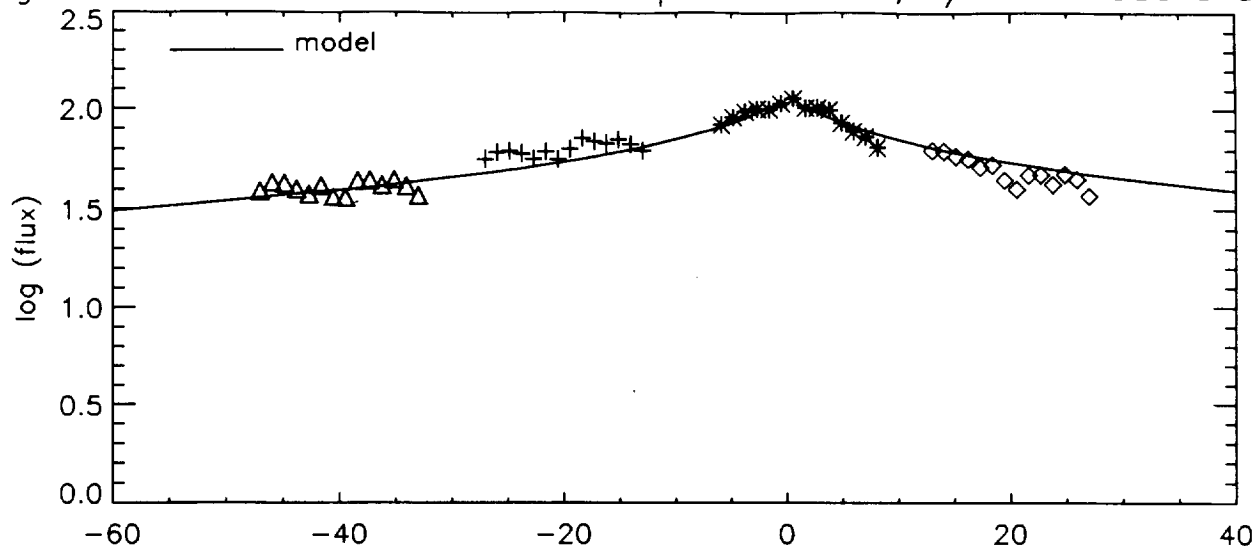
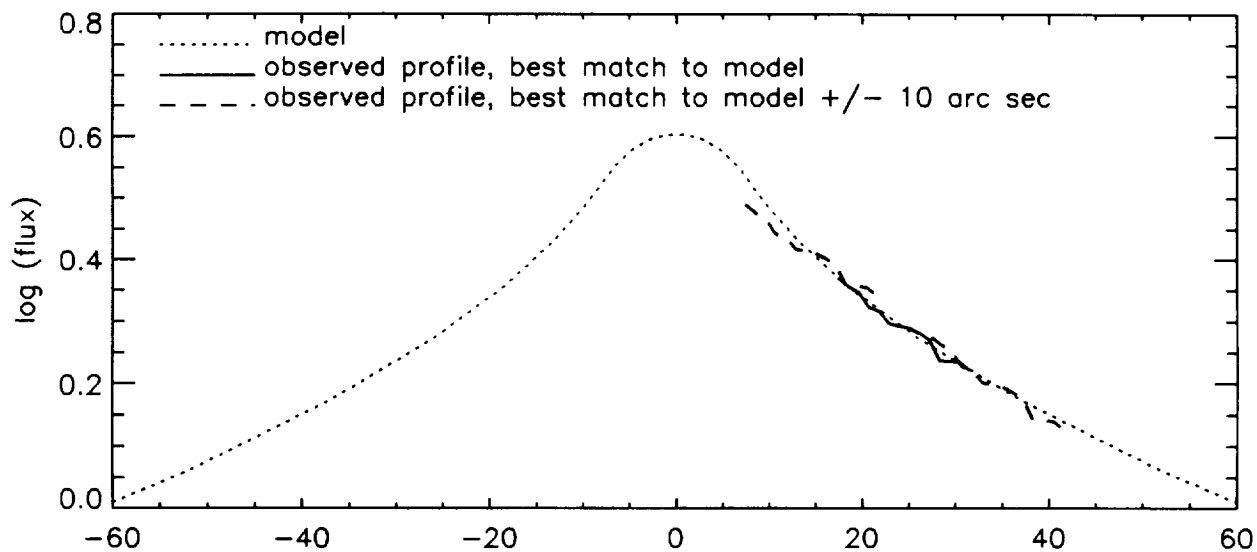


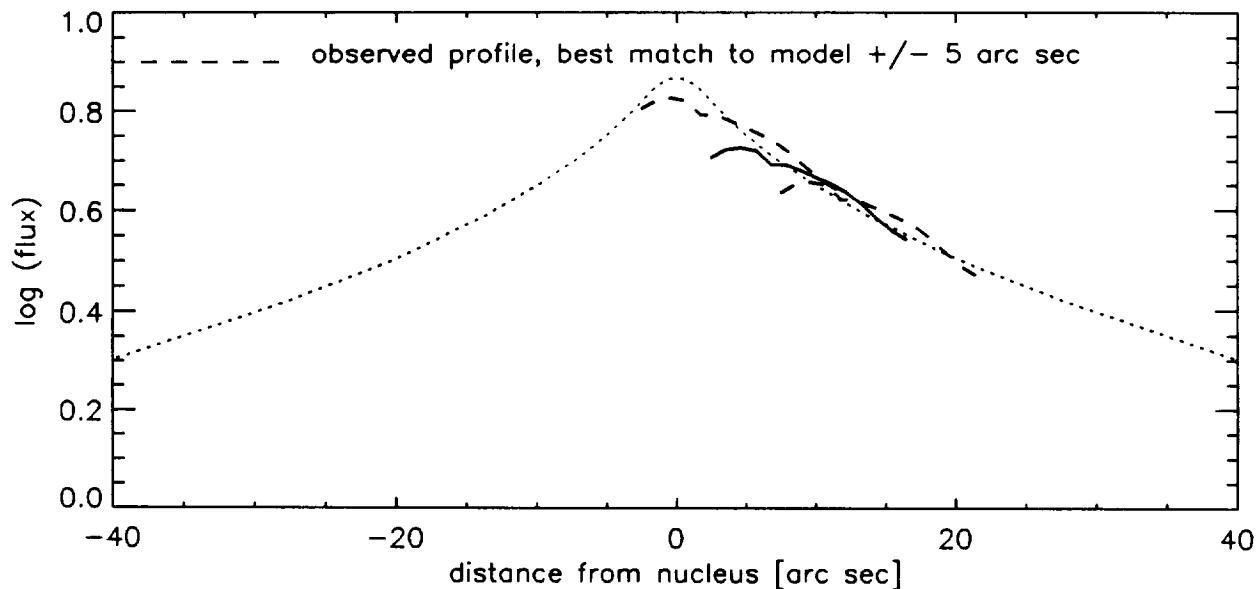
Figure 2 – Model and Observed IUE Spatial Profiles, P/Encke 1980 and 1990



a.) Composite Spatial Profile Nov 04 1980



b.) LWP 18833



c.) LWP 18881

Figure 3 – H₂O Production, 2P/Encke and 9P/Tempel 1, from IUE OH Data

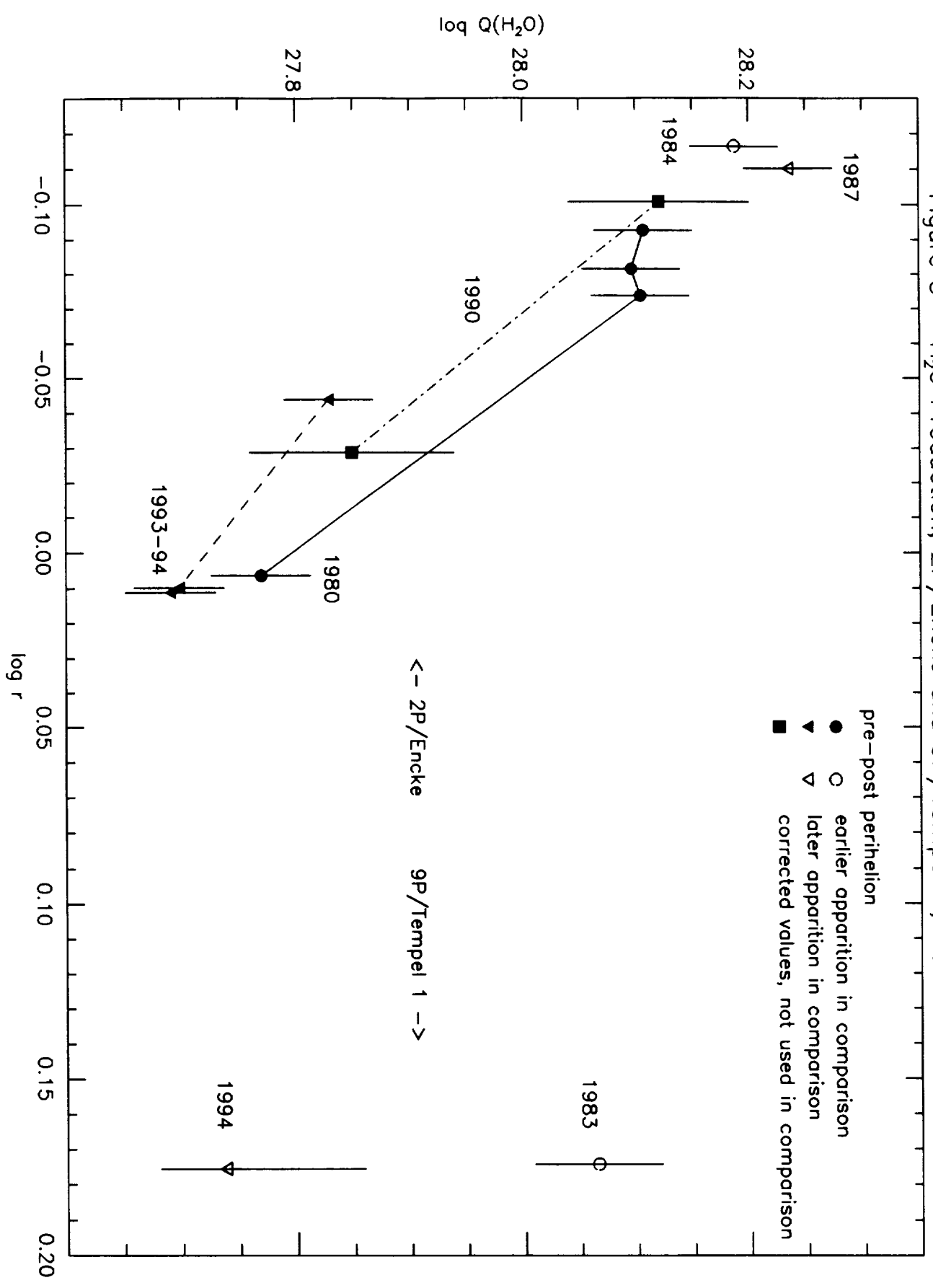


Table 1
IUE Observations

Image	Date	Exposure [min]	v^\dagger [deg]	ΔT^\ddagger [day]	r [AU]	Δ [AU]	\dot{r} [km/s]
<u>P/Encke</u>							
<u>Pre-perihelion</u>							
LWR09135*	1980 Oct 24.333	60	-116.757	-43.2	1.015	0.291	-28.42
LWR09218	1980 Nov 03.364	30	-107.630	-33.2	0.844	0.300	-30.33
LWR09224	1980 Nov 04.224	30	-106.673	-32.4	0.829	0.308	-30.49
LWR09234	1980 Nov 05.230	20	-105.504	-31.3	0.808	0.319	-30.71
LWP18833	1990 Sep 20.226	60	-114.008	-38.3	0.936	0.829	-29.57
LWP18881	1990 Sep 28.383	30	-105.544	-30.2	0.793	0.797	-31.18
LWP27120*	1993 Dec 27.795	60	-118.293	-43.7	1.026	0.923	-28.50
LWP27121*	1993 Dec 27.944	100	-118.183	-43.5	1.023	0.922	-28.53
LWP27160	1994 Jan 04.019	30	-112.287	-36.5	0.904	0.887	-29.95
<u>Post-perihelion</u>							
LWP03217*	1984 Apr 25.467	90	+102.107	+28.8	0.765	0.763	+31.06
LWP11402*	1987 Aug 15.650	10	+104.227	+29.3	0.776	0.885	+31.32
<u>P/Tempel 1 Post-perihelion</u>							
LWR16372*	1983 July 19.095	120	+6.196	+9.3	1.494	1.003	+1.11
LWP28634*	1994 July 14.404	240	+7.366	+11.1	1.498	0.914	+1.32

(* = used in comparison)

† true anomaly

‡ time from perihelion

Table 2 - IUE Results

Image	B(0-0) [R]	B(Q=10 ²⁸) from model	Q _{H2O} 10 ²⁸ mol/sec	Q _{later} /Q _{earlier}
<u>P/Encke (only observations at comparable r)</u>				
<u>Pre-perihelion</u>				
¹⁹⁸⁰ LWR09135	3162 ±190	5382	0.588 ±0.057	
¹⁹⁹³ LWP27120	1634 ±82	2549	0.490 ±0.044	
¹⁹⁹³ LWP27121	1704 ±85	2609	0.499 ±0.045	(85±11)%
<u>Post-perihelion</u>				
¹⁹⁸⁴ LWP03217	687 ±21	543	1.27 ±0.10	
¹⁹⁸⁷ LWP11402	694 ±42	471	1.47 ±0.14	(116±14)%
<u>P/Tempel 1 Post-perihelion</u>				
¹⁹⁸³ LWR16372	539 ±32	651	0.828 ±0.079	
¹⁹⁹⁴ LWP28634	236 ±12	646	0.365 ±0.033	(44±6)%
(corrected)	271 ±14	646	0.420 ±0.038	(51±7)%